The Temperature and Coverage Dependences of Adsorbed Formic Acid and Its Conversion to Formate on Pt(111)

ARTICLE *in* JOURNAL OF THE AMERICAN CHEMICAL SOCIETY · FEBRUARY 1992

Impact Factor: 12.11 · DOI: 10.1021/ja00030a017

3 AUTHORS, INCLUDING:

Patricia A Thiel
Iowa State University
350 PUBLICATIONS **9,462** CITATIONS

SEE PROFILE

amide anion, to shift the equilibrium by at least 17 kcal/mol!

Arnett and Moe have measured the enthalpies of reaction for **2b** reacting with a number of acids in THF solvent,[4] as well as for a number of lithiated species reacting with 2-propanol in 90% hexane/10% diethyl ether.[8] If these enthalpies are plotted versus the gas-phase enthalpies of acidity,[21] as shown in Figures 2 and 3, it is evident that there is a general parallel trend in the two phases. For a given functional group, such as the alkyl- and dialkylamines in Figure 2, the largest substituents result in the amine being the least acidic in solution, but the most acidic in the gas phase, consistent with polarizability and solvation effects.[22,14] The position of **2a** is anomalous in these plots: it is considerably more weakly acidic in solution than expected from the gas-phase data and well removed from the other amine acids. This is further evidence for very different structures of **2b** and **2c**.

Such a change in reactivity based on the counterion implies that proper choice of solvent and/or counterion may allow considerable selectivity in this case. An example is the relative basicities of the sodium salt of **2c** vs the lithium salt **2b**; the latter resulted in only γ-deprotonation of an α,β unsaturated ketone, but the sodium salt deprotonated an adjacent simple ketone in the same molecule.[2] Although kinetic control may be invoked as the difference here, the counterion may be controlling the equilibria at the stage of the initial proton transfer, since the γ site of the conjugated enone is comparable in intrinsic acidity to that of the amide anion.[41]

The anions of the trialkylsilanols have been used in solution primarily as nucleophiles which are the synthetic equivalent of O^{2-}.[42] The observed basicity, in that R_3SiO^- does not deprotonate the α-H of esters in solution, is consistent with the anion's weak basicity in the gas phase.

Conclusions

Knowledge of the intrinsic reactivity of species of this type, plus observing how this can be subsequently modified by solvation and counterions, allows the chemist better control and selection of the available reaction pathways. It has been shown that the observed reactivity of dialkylamide anions in solution is consistent with their intrinsic reactivity, but that hexamethyldisilazide anion appears to have its solution phase reactivity modified considerably by the counterion. Further exploration of counterion effects on the reactivity of **2c**, or possibly of species of the type Me_3Si–NHR, where R = some bulky alkyl group, would be of interest. The latter species should be intrinsically just a little weaker in acidity than any ester or ketone, so that counterion control might tune its reactivity through the range of synthetic interest.

Acknowledgment. We thank Professor E. M. Arnett for sharing his results with us prior to publication and NSF for support.

Registry No. 1a, 108-18-9; **1b**, 414-54-0; **1c**, 94612-69-8; **2a**, 999-97-3; **2b**, 4039-32-1; **2c**, 92231-05-5; **3a**, 768-66-1; **3b**, 38227-87-1; **3c**, 138054-31-6; **4**, 597-52-4; Me_2NH, 124-40-3; Me_3SiNH_2, 7379-79-5; Me_3SiOH, 1066-40-6; lithium ion(+), 17341-24-1.

(41) Bartmess, J. E.; Kiplinger, J. P. *J. Org. Chem.* **1986**, *51*, 2173.

(42) Laganis, E. D.; Chenard, B. L. *Tetrahedron Lett.* **1984**, *28*, 5831.

The Temperature and Coverage Dependences of Adsorbed Formic Acid and Its Conversion to Formate on Pt(111)

M. R. Columbia, A. M. Crabtree, and P. A. Thiel*,†

Contribution from the Department of Chemistry and Ames Laboratory, Iowa State University, Ames, Iowa 50011. *Received May 28, 1991*

Abstract: We have studied the adsorption of HCOOH on Pt(111) at 80–100 K and its conversion to formate with increasing surface temperature. The techniques employed are thermal desorption spectroscopy and high-resolution electron energy loss spectroscopy. At very low exposures (<0.2 langmuir), we posit that HCOOH exists molecularly as monomers or discrete dimer pairs. As exposure increases, there is evidence for hydrogen-bonded chains with the molecular plane of HCOOH nearly parallel to the surface. At an exposure of 0.2 L, these chains resemble the solid-phase β-polymorph as indicated by the vibrational frequencies of the OH out-of-plane bending vibration. Heating this surface causes the chains to break apart into discrete dimer pairs, followed by deprotonation to a bridging formate adspecies. The formate decomposes between 210 K and 280 K, causing CO_2 desorption and leaving hydrogen adatoms. Increasing the exposure above 0.6 L causes the chains to adopt a structure similar to the denser α-polymorph. Heating this surface causes molecular desorption in two states. One is centered at 160 K and is dominated by gaseous HCOOH dimers. Desorption in this state leaves bridging formate and β-polymorphic HCOOH coexistent on the surface. The other is centered at 200 K and is primarily gaseous monomers. Desorption in this state leaves only the formate adspecies. Its decomposition then proceeds as on the surface exposed to 0.2 L HCOOH.

1. Introduction

The adsorption of formic acid (HCOOH) on transition metal surfaces and its subsequent reactions are of ongoing interest within the surface scientific community. The majority of studies focus on the decomposition intermediates of the acid and their ultimate products.[1-18] Decomposition can occur via dehydrogenation, as on Pt[1-4] and Cu,[5-7] or by a combination of dehydrogenation and dehydration, as on Ni[8-15] and Ru.[16-18] The most commonly observed intermediate is formate in a bridging configuration (bonding through the oxygen atoms to two surface atomic sites), although

† National Science Foundation Presidential Young Investigator (1985–89) and Camille and Henry Dreyfus Foundation Teacher–Scholar (1986–90).

(1) Columbia, M. R.; Thiel, P. A. *Surf. Sci.* **1990**, *235*, 53.
(2) Avery, N. R. *Appl. Surf. Sci.* **1982**, *11/12*, 774.
(3) Avery, N. R. *Appl. Surf. Sci.* **1982–83**, *14*, 149.
(4) Abbas, N.; Madix, R. J. *App. Surf. Sci.* **1983**, *16*, 424.
(5) Ying, D. H. S.; Madix, R. J. *J. Catal.* **1980**, *61*, 48.
(6) Hayden, B. E.; Prince, K.; Woodruff, D. P.; Bradshaw, A. M. *Surf. Sci.* **1983**, *133*, 589.
(7) Dubois, L. H.; Ellis, T. H.; Zegarski, B. R.; Kevan, S. D. *Surf. Sci.* **1986**, *172*, 385.
(8) McCarty, J.; Falconer, J.; Madix, R. J. *J. Catal.* **1973**, *30*, 235.

0002-7863/92/1514-1231$03.00/0

formic anhydride has recently been identified on Ni(111) using IR spectroscopy.[15]

Far fewer studies deal with the topic of this paper, molecular adsorption of HCOOH and its conversion to formate.[19-23] These studies involve more inert metals such as Ag[19,20] and Au.[21,22] Thermal desorption from these surfaces shows only molecular desorption, which appears in two states at 160–180 K and 190–210 K, attributed to multilayer and first layer desorption, respectively. High-resolution electron energy loss (HREEL) spectra show that conversion to formate occurs in the presence of coadsorbed atomic oxygen, but no HREEL spectra have been reported for formate on the clean surfaces of these metals. Vibrational spectra of the molecular acid indicate that, upon adsorption, the molecules form hydrogen-bonded structures similar to gas-phase dimers on Cu(100)[6] and Au(111)[21] and solid-phase catameric chains on Pt(111)[2] and Au(110).[21] Vibrational spectra of acetic acid adsorbed on Pd(111)[24] and Pt(111)[25,26] show evidence of similar hydrogen-bonded structures.

Joyner and Roberts[23] have used photoelectron spectroscopy to compare acid-to-formate conversion on polycrystalline surfaces of Cu, Ni, and Au. They demonstrate similar temperature-dependent changes in the photoelectron spectra for HCOOH on all three metals. Their subsequent interpretation presents a common scheme of molecular acid-to-formate conversion involving (1) the formation of hydrogen-bonded chains following adsorption at 80 K, (2) the breaking of hydrogen bonds between 120 K and 150 K, and (3) the loss of the hydroxyl proton to the surface accompanied by reorientation to give a formate adspecies with its molecular plane perpendicular to the surface between 150 K and 170 K. This adspecies is stable on Cu and Ni, eventually decomposing to give CO_2 and H_2; however, owing to its lower stability on Au, recombinative desorption occurs instead above 170 K.

We have studied the interaction of HCOOH with clean Pt(111) using thermal desorption spectroscopy (TDS) and high-resolution electron energy loss spectroscopy (HREELS) in order to better characterize the coverage and temperature dependence of the molecular acid-to-formate conversion on this surface. We have previously reported desorption of molecular HCOOH and decomposition products (CO_2 and H_2) from a saturated first layer, as well as additional molecular desorption states for higher exposures.[1,27] We now present detailed models to explain this desorption behavior and the observed temperature- and coverage-dependent changes in our HREEL spectra based on comparison to vibrational spectra of HCOOH in the gas phase[28,29] and solid phase,[29-31] as well as adsorbed formate on Pt(111).[2,3]

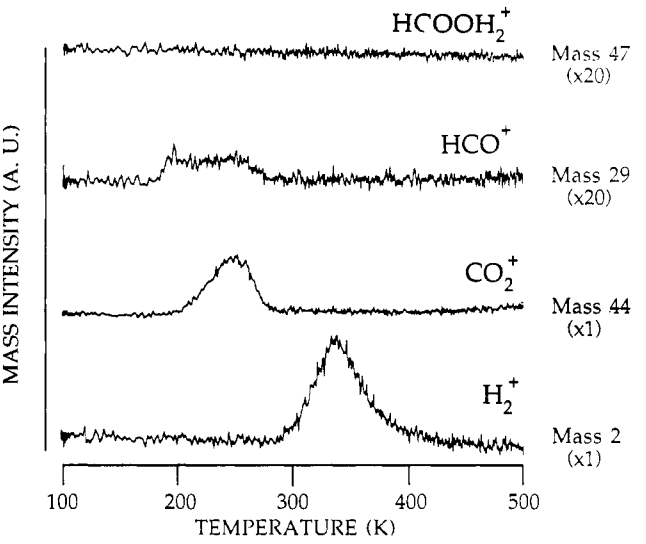

Figure 1. Thermal desorption traces of H_2^+, CO_2^+, HCO^+, and $HCOOH_2^+$ following exposure of 0.2 L HCOOH at 80–100 K. The heating rate is 6.2 K/s at 100 K and drops continuously to 1.9 K/s at 500 K. (HCO^+ monitors monomeric HCOOH desorption and $HCOOH_2^+$ monitors dimeric HCOOH desorption.)

2. Experimental Details

The ultrahigh vacuum system, the method of performing thermal desorption experiments, and the Pt(111) crystal used for these experiments have been previously outlined.[1,32,33] The exposure units reported in this paper are langmuir (L), although the surface is exposed to HCOOH through a directional doser containing a conductance-limiting aperture. We determine the langmuir equivalence of these exposures by comparing CO thermal desorption areas for exposure via the doser with areas for exposure via backfilling. The conductance of the limiting aperture allows pressures of 100 mTorr to be used in the dosing line; this ensures that HCOOH exposed to the Pt(111) surface is primarily monomeric.[34] We desire this condition to avoid the complications which arise from adsorption of dimeric HCOOH reported by Benziger and Schoofs on Ni(111).[14]

The high-resolution electron energy loss spectrometer has also been described previously.[33] The elastic peaks for the experiments we report here have intensities between 50 kHz and 350 kHz and full-widths at half-maxima between 8 and 11 meV (65 cm^{-1} to 89 cm^{-1}). For those experiments which probe the effect of temperature on the vibrational spectrum, exposure temperatures are between 80 K and 100 K; the surface is then heated to the indicated temperature at ~5 K/s, followed by determination of the loss spectrum while the surface cools. This method of heating differs from the continuous heating performed in TDS experiments. Because of this, desorption states occur at higher temperatures (by 10–20 K) than the corresponding changes in the vibrational spectrum.

3. Results

1. Thermal Desorption. In previous work[1,27] we have shown that the sequence of appearance of desorption products with increasing HCOOH exposure is (1) H_2 and CO_2, (2) HCOOH at 200 K, (3) HCOOH at 160–170 K, and (4) HCOOH at 160 K. The first three sets of desorption products each saturate at about the point where the next appears. We observe only H_2 and CO_2 at exposures below 0.3 L; the molecular acid state at 200 K develops between 0.3 and 0.6 L; that at 160–170 K develops between 0.6 and 1.2 L; and a final molecular state at 160 K appears at 1.2 L, then grows without limit. The behavior of the

(9) Falconer, J. L.; Madix, R. J. *Surf. Sci.* **1974**, *46*, 473.
(10) Madix, R. J.; Gland, J. L.; Mitchell, G. E.; Sexton, B. A. *Surf. Sci.* **1983**, *125*, 481.
(11) Jones, T. S.; Richardson, N. V.; Joshi, A. W. *Surf. Sci.* **1988**, *207*, L948.
(12) Jones, T. S.; Ashton, M. R.; Richardson, N. V. *J. Chem. Phys.* **1989**, *90*, 7564.
(13) Benziger, J. B.; Madix, R. J. *Surf. Sci.* **1979**, *79*, 394.
(14) Benziger, J. B.; Schoofs, G. B. *J. Phys. Chem.* **1984**, *88*, 4439.
(15) Erley, W.; Sander, D. *J. Vac. Sci. Technol. A* **1989**, *7*, 2238.
(16) Larson, L. A.; Dickinson, J. T. *Surf. Sci.* **1979**, *84*, 17.
(17) Avery, N. R.; Toby, B. H.; Anton, A. B.; Weinberg, W. H. *Surf. Sci.* **1982**, *122*, L574.
(18) Sun, Y.-K.; Weinberg, W. H. *J. Chem. Phys.* **1991**, *94*, 4587.
(19) Barteau, M. A.; Bowker, M.; Madix, R. J. *Surf. Sci.* **1980**, *94*, 303.
(20) Sexton, B. A.; Madix, R. J. *Surf. Sci.* **1981**, *105*, 177.
(21) Chtaib, M.; Thiry, P. A.; Pireaux, J. J.; Delrue, J. P.; Caudano, R. *Surf. Sci.* **1985**, *162*, 245.
(22) Outka, D. A.; Madix, R. J. *Surf. Sci.* **1987**, *179*, 361.
(23) Joyner, R. W.; Roberts, M. W. *Proc. R. Soc. London, Ser. A* **1976**, *350*, 107.
(24) Davis, J. L.; Barteau, M. A. *Langmuir* **1989**, *5*, 1299.
(25) Gao, Q.; Hemminger, J. C. *J. Electron Spectrosc.* **1990**, *54/55*, 667.
(26) Gao, Q.; Hemminger, J. C. *Surf. Sci.* **1991**, *248*, 45.
(27) Columbia, M. R.; Thiel, P. A. *Proceedings of the DOE Workshop-Direct Methanol/Air Fuel Cells: 1990*, to be published.
(28) Millikan, R. C.; Pitzer, K. S. *J. Chem. Phys.* **1957**, *27*, 1305.
(29) Millikan, R. C.; Pitzer, K. S. *J. Am. Chem. Soc.* **1958**, *80*, 3515.
(30) Mikawa, Y.; Jakobsen, R. J.; Brasch, J. W. *J. Chem. Phys.* **1966**, *45*, 4750.
(31) Mikawa, Y.; Brasch, J. W.; Jakobsen, R. J. *J. Mol. Spectrosc.* **1967**, *24*, 314.
(32) Columbia, M. R.; Thiel, P. A. *Rev. Sci. Instrum.* **1987**, *58*, 309.
(33) Leavitt, P. K.; Davis, J. L.; Dyer, J. S.; Thiel, P. A. *Surf. Sci.* **1989**, *218*, 346.
(34) Cooley, A. S. *J. Am. Chem. Soc.* **1928**, *50*, 2166.

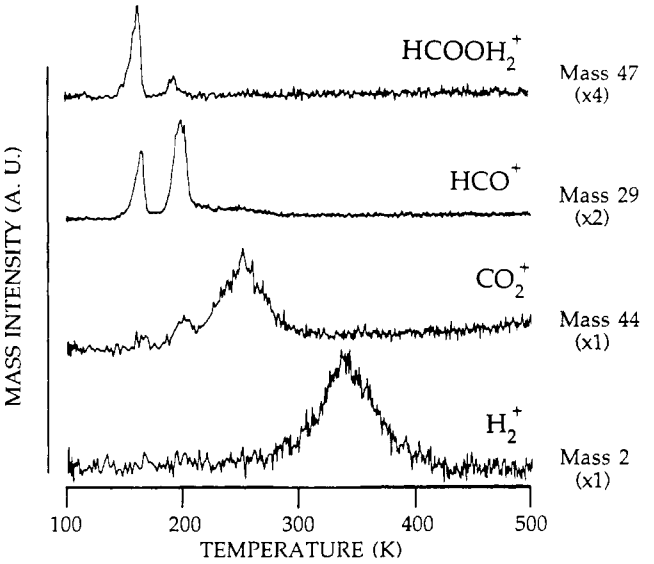

Figure 2. Thermal desorption traces of H_2^+, CO_2^+, HCO^+, and $HCOOH_2^+$ following exposure of 0.8 L HCOOH at 80–100 K. The heating rate is 6.2 K/s at 100 K and drops continuously to 1.9 K/s at 500 K. (HCO^+ monitors monomeric HCOOH desorption and $HCOOH_2^+$ monitors dimeric HCOOH desorption.) The small offset between the mass 47 and 29 peaks at 160 K may be an experimental artifact; the larger offset at 200 K probably indicates that dimer desorption precedes monomer desorption in this state.

latter suggests that it is a multilayer state. The two exposures which are emphasized in this paper, 0.2 and 0.8 L, fall in the first and third adsorption regimes; they are 0.7 and 2.7 times the exposure necessary to saturate the dissociation products, H_2 and CO_2. Direct measurements of coverage versus exposure have not been made for this system, and so we present our data in terms of exposures only; all evidence supports the assumption, however, that coverage is an increasing function of exposure at 80–100 K.

Figures 1 and 2 display thermal desorption spectra for masses 2, 44, 29, and 47 for Pt(111) exposed to 0.2 L and 0.8 L HCOOH, respectively. For an exposure of 0.2 L, all adsorbed HCOOH converts to formate. In Figure 1 we observe primarily the decomposition products CO_2 and H_2. The CO_2 desorption peaked at 260 K is attributed to the decomposition of a surface formate species at 210–280 K with the remaining H adatoms desorbing at 300–400 K, a temperature similar to that observed for a Pt(111) surface exposed only to H_2.[35] A small amount of molecular desorption occurs between 200 K and 250 K (mass 29 spectrum); this is most probably recombination of surface formate with H adatoms. The mass 47 spectrum has no features at this exposure.

For 0.8 L exposure the surface produces molecular desorption, as well as CO_2 and H_2 desorption. At this exposure, features at 160 K and 200 K in the spectra for masses 29 and 47 (Figure 2) indicate molecular desorption. There is a marked difference in these spectra regarding the intensities of these features. In the mass 29 spectrum, the 200 K feature is the more intense with three times the desorption area of the 160 K feature. Just the opposite occurs in the mass 47 spectrum with the 160 K spectrum having a desorption area six times that of the 200 K feature. There is little change in the desorption features for masses 44 and 2.

2. High-Resolution Electron Energy Loss Spectroscopy. Figures 3 and 4 show HREEL spectra which contain all loss features observed in this system, thus serving as a basis for the mode assignments. Figure 3 is obtained after exposing Pt(111) to 0.8 L HCOOH followed by heating to 130 K. Under these conditions, we assign all loss features to molecularly adsorbed acid. At 130 K there is better surface ordering than at 80–100 K (ascertained from the quality of the elastic conditions for the two temperatures), but the heating produces no desorption from the surface. Figure 4 shows the HREEL spectrum for the same exposure followed by heating to 190 K. By this temperature molecular desorption is complete; all remaining loss features can be assigned to adsorbed formate.

(35) Christmann, K.; Ertl, G.; Pignet, T. *Surf. Sci.* **1976**, *54*, 365.

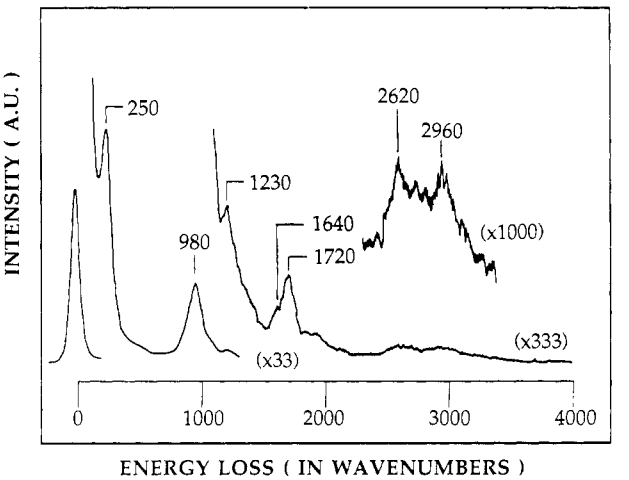

Figure 3. High-resolution electron energy loss spectrum following exposure of 0.8 L HCOOH at 80–100 K and heating to 130 K. The elastic peak has an intensity of 350 kHz and a fwhm of 9 mV.

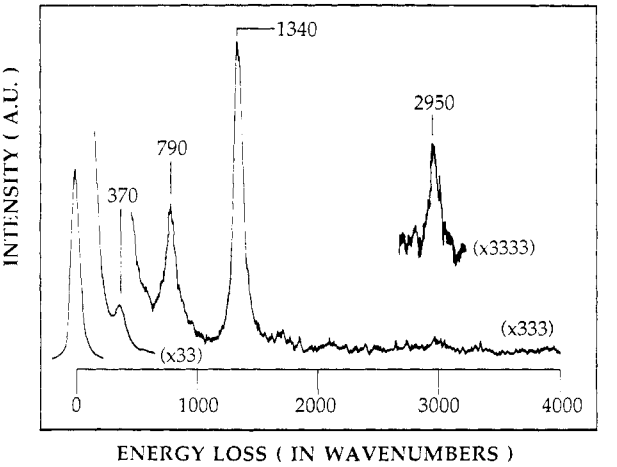

Figure 4. High-resolution electron energy loss spectrum following exposure of 0.8 L HCOOH at 80–100 K and heating to 190 K. The elastic peak has an intensity of 110 kHz and a fwhm of 10 mV.

Table I. Loss Assignments for High-Resolution Electron Energy Loss Spectra of Molecular HCOOH (Figure 3) and Bridging Formate (Figure 4) on Pt(111)[a]

formic acid		formate	
loss	mode	loss	mode
250	lattice	370	ν(PtO)
980	π(OH)	790	δ(OCO)
1230	ν(C—O)	1340	ν_s(OCO)
1640	ν(C=O)	2950	ν(CH)
1720	ν(C=O)		
2620	ν(OH)		
2960	ν(CH)		

[a] Mode determination made by comparison to Avery.[2]

Assignments of the prominent losses are based upon comparison to Avery[2] and are summarized in Table I for molecular HCOOH (Figure 3) and bridging formate (Figure 4). Avery argues convincingly for the assignment of the formate losses to a bridging, rather than mono- or bidentate species; the molecular acid adsorbs in a layer structure with the molecular plane nearly parallel to the surface. The similarity between our data and his suggests that the same interpretations are valid here.

For the molecular acid, we do not observe losses at 715 cm^{-1} (δ(OCO), 1070 cm^{-1} (π(CH)), and 1385 cm^{-1} (δ(CH)) reported by Avery; this can be explained by a higher HCOOH coverage

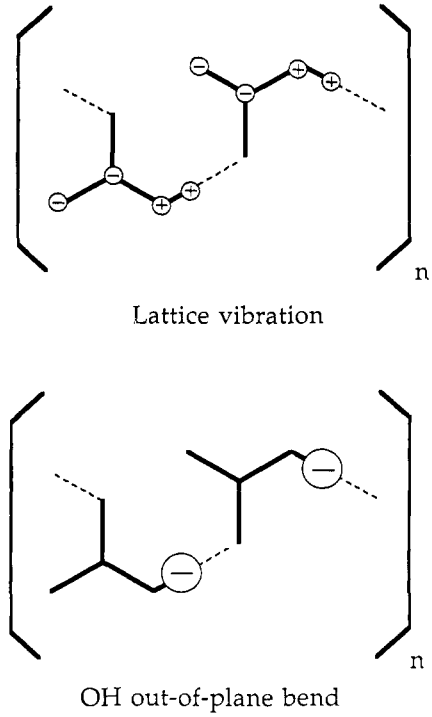

Figure 5. Geometric representations of solid HCOOH lattice vibration and OH out-of-plane bend. (+) and (−) signify displacement of atoms above and below the molecular plane, respectively (taken from Mikawa et al.[31]).

and better resolution in Avery's work. The in-plane bending modes (δ) produce relatively small dipole changes perpendicular to the surface resulting in small dipolar scattering cross sections; higher coverages are required to observe them. The low intensity of the π(CH) vibration, the out-of-plane deformation, is unexpected based on the adsorption geometry but is consistent with a strong impact scattering contribution observed for ν(CH) for formate adsorbed on Pt(110)[36] and Ni(110).[12]

The most intense losses for this overlayer are assigned to out-of-plane vibrations: a lattice vibration at 250 cm^{-1} and the out-of-plane OH deformation at 980 cm^{-1}. We illustrate these vibrations in Figure 5.

The molecular HCOOH loss at 250 cm^{-1} assigned to a lattice vibration has been used previously as an indication of multilayer population.[20] However, we observe this loss clearly for exposures as low as 0.3 L, which is insufficient to populate any multilayer-like desorption state on Pt(111) (data not shown). Instead, we believe the adsorbed HCOOH layer consists of quasi-one-dimensional chains with practically no interaction between chains. This loss, as assigned by Mikawa et al.,[31] then results from simultaneous displacement of the hydroxyl oxygen atom and its proton above the molecular plane, and the carbon atom and its proton below it, as shown in Figure 5.

The splitting of the ν(C=O) mode and the frequency of the π(OH) mode also give information about the structure of the molecular acid. The π(OH) frequency is higher than those of monomeric or dimeric HCOOH (see Table II). It is much closer to those measured for solid HCOOH, which exists in two polymorphic structures.[30,31] The α-polymorph exhibits tautomerism giving rise to two ν(C=O) modes; the β-polymorph exhibits no tautomerism and only one ν(C=O) mode. The splitting in our spectrum indicates that we, like Avery, observe an overlayer structure similar to the HCOOH α-polymorph. (This is also supported by the π(OH) frequency.) The consequences of polymorphism on surface adstructure are discussed later.

Sequential heating-measurement cycles allow correlation of surface changes with desorption states. Figure 6 displays a series

(36) Hofmann, P.; Bare, S. R.; Richardson, N. V.; King, D. A. *Surf. Sci.* **1983**, *133*, L459.

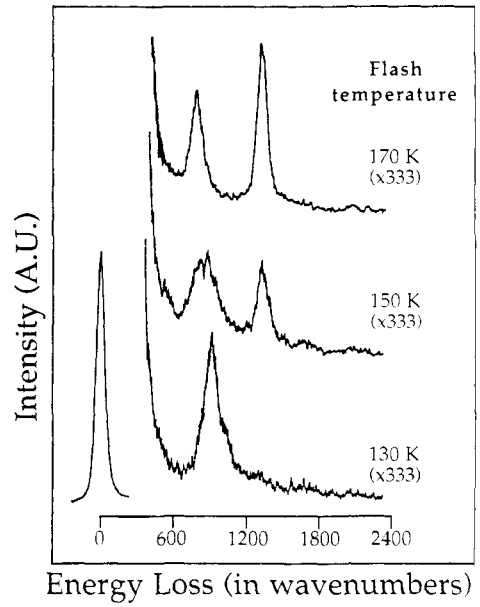

Figure 6. Series of high-resolution electron energy loss spectra following exposure of 0.2 L HCOOH at 80–100 K and heating to 130 K, 150 K, and 170 K, respectively. The elastic peak has an intensity of 50 kHz and a fwhm of 11 mV.

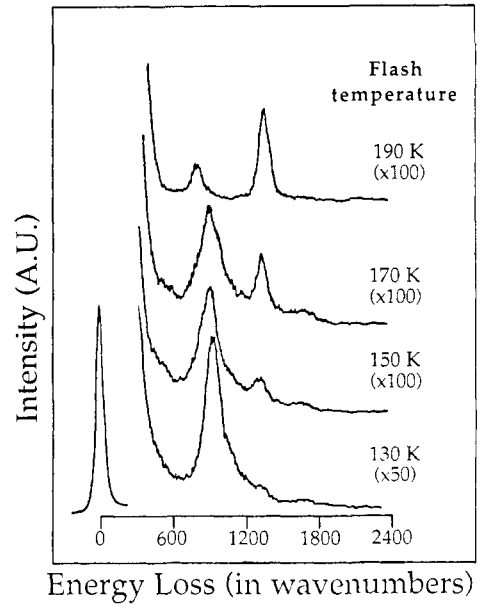

Figure 7. Series of high-resolution electron energy loss spectra following exposure of 0.8 L HCOOH at 80–100 K and heating to 130 K, 150 K, 170 K, and 190 K, respectively. The elastic peak has an intensity of 100 kHz and a fwhm of 8 mV.

of HREEL spectra obtained after exposing Pt(111) to 0.2 L HCOOH followed by heating to 130 K, 150 K, and 170 K. The only prominent loss in the 130 K spectrum occurs at 940 cm^{-1}. We assign this to the OH out-of-plane bend for the molecular HCOOH and note that it shifts down by 40 cm^{-1} relative to the spectrum in Figure 3. In the 150 K spectrum this loss shifts further down to ca. 900 cm^{-1} and decreases in intensity; new losses appear at 790 cm^{-1} and 1340 cm^{-1}, indicating the presence of bridging formate. By 170 K the spectrum exhibits only the losses from the formate adspecies.

Figure 7 shows an HREEL spectral series obtained after exposing Pt(111) to 0.8 L HCOOH followed by heating to 130 K, 150 K, 170 K, and 190 K. The only prominent loss observed in the spectrum at 130 K occurs at 980 cm^{-1}, agreeing with the OH out-of-plane bend for molecular HCOOH in Figure 3. The 150 K spectrum shows that this loss shifts down to 945 cm^{-1} and decreases in intensity, while a new loss at 1330 cm^{-1} appears

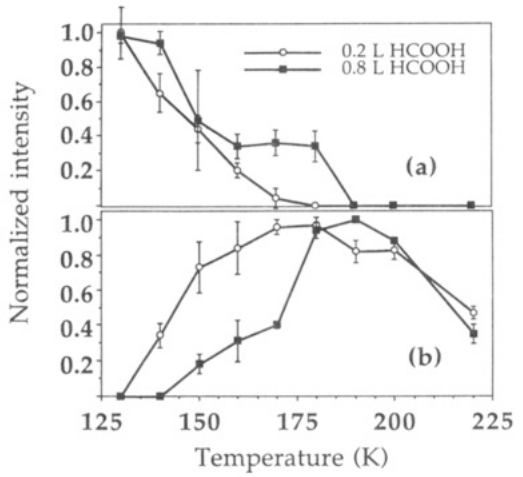

Figure 8. (a) Loss intensity of the HCOOH out-of-plane OH bend normalized to the elastic intensity as a function of temperature for exposures of 0.2 L and 0.8 L. (b) Loss intensity of the formate OCO symmetric stretch normalized to the elastic intensity as a function of temperature for exposures of 0.2 L and 0.8 L. Each normalized value is the average of three to five measurements made after heating to the stated temperature and the error bars reflect ±1 standard deviation.

indicating the presence of bridging formate. The 170 K spectrum shows an increase for the formate loss intensity but little change in the molecular HCOOH loss. By 190 K the spectrum exhibits no losses for molecular HCOOH and a new loss at 790 cm^{-1}; this spectrum is in good agreement with the one in Figure 4 where only bridging formate is present on the surface.

In Figure 8, a and b depict the conversion of molecular HCOOH to formate in a graphical manner. In Figure 8a the loss intensity of the OH out-of-plane bend for molecular HCOOH normalized to the elastic intensity is plotted versus surface temperature for 0.2 L and 0.8 L HCOOH exposures. For the lower exposure there is a constant intensity decrease to extinction between 170 K and 180 K; however, the intensity decrease for the higher exposure produces a plateau between 160 K and 180 K before extinction at 190 K. In Figure 8b the normalized loss intensity for the OCO symmetric stretch for the bridging formate is plotted versus temperature for the same exposures. For the lower exposure, the intensity increases rapidly between 130 K and 150 K and reaches a maximum around 180 K. This increase occurs more slowly at the higher exposure up to 170 K; beyond this temperature the intensity increases rapidly to its maximum at 190 K.

4. Discussion

1. Temperature and Coverage Dependence of the OH Out-of-Plane Bend Frequency. In the HREEL spectra for conditions where molecular HCOOH exists on the surface, the most intense loss belongs to the OH out-of-plane bend. The frequency of this loss occurs in three distinct ranges depending on the exposure and surface temperature. These frequencies and the conditions where we observe them are listed in Table II along with frequencies for various forms of molecular HCOOH. The monomer and dimer frequencies are available for those species in the gas phase;[28,29] the alpha (α) and beta (β) polymorph frequencies are available for solid HCOOH.[29-31] The vibrational frequencies for the different forms of formic acid increase with increasing strength of hydrogen bonding; this is in accord with Novak's review of several molecules which exhibit hydrogen-bonding in the solid phase.[37] Rough molecular models are also shown for each of these forms accompanying the appropriate π(OH) frequency.

For the 0.8 L exposure heated to 130 K, the OH bend has an average frequency of 978 cm^{-1}, the same frequency as the α-polymorph; heating to 150 K causes the average frequency to shift to 945 cm^{-1}, close to the frequency of the β-polymorph. In Figure 9 we display possible structures for these polymorphs as they might exist on the Pt(111) surface. We construct these by attempting to maximize symmetry and registry with the surface. This requires lengthening the (OH–O) bond distances from 0.258 nm to 0.277 nm. No bond angles are distorted beyond reported uncertainty.[38]

(37) Novak, A. *Struct. Bonding (Berlin)* **1974**, *18*, 177.

Table II. Frequencies (in Wavenumbers) for the OH Out-of-Plane Bend of Molecular HCOOH[a]

HCOOH π (OH) frequency (wavenumbers)	
Monomer	636
Dimer	917
α-polymorph	974
β-polymorph	947

Adspecies π (OH) loss (wavenumbers)	
0.8 L HCOOH @ 130 K	978 ± 11
0.8 L HCOOH @ 150 K	945 ± 4
0.2 L HCOOH @ 130 K	938 ± 4
0.2 L HCOOH @ 150 K	898 ± 4

[a] The values for the monomer and dimer are reported for the gas phase,[28,29] and those for the two polymorphs are reported for solid HCOOH.[29-31] The adspecies' values are averages of five to seven measurements for each surface condition described.

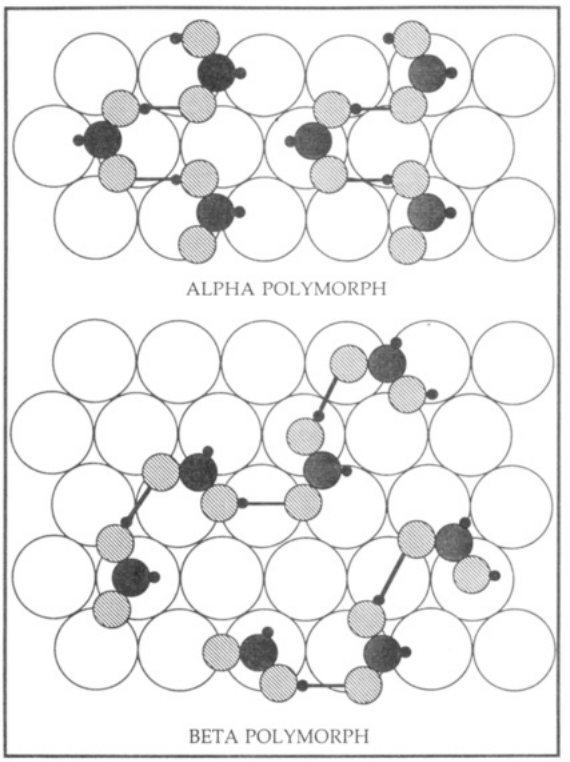

Figure 9. Models of HCOOH overlayer structures on Pt(111) are based on the solid phase α- and β-polymorphs. These models are constructed by elongating each O–H–O hydrogen bond distance from 0.258 nm to match the Pt–Pt distance on the (111) surface, 0.277 nm, and positioning the oxygen atoms in 2-fold hollow or on-top sites. Interchain distances do not allow atoms in different chains to approach closer than 0.368 nm center to center. No bond angles are distorted beyond reported uncertainty.[38]

It is easily observed, qualitatively and quantitatively, that the α-phase is the denser of the two polymorphs. The absolute coverages of the α- and β-polymorphs, as shown in Figure 9, are 0.3 and 0.2 monolayer, respectively. These values are based on the shortest interchain distance which maintains registry with the surface and provides good agreement with the same distances in solid HCOOH.[38] These distances between chains in the bulk solid are 0.375 nm for C–C separation, 0.328 nm for O–O separation, and 0.318 nm for C–O separation; in Figure 9, the shortest interchain distance is the C–C separation for the α-polymorph at 0.368 nm and the O–O separation for the β-polymorph at 0.368 nm. We interpret the frequency shift as function of temperature to indicate a transition of the molecular HCOOH from the α-polymorph at 130 K to the β-polymorph at 150 K. Such a transition results in displacement of HCOOH molecules from direct contact with the surface and could explain the 160 K molecular desorption state at this exposure.

For the 0.2 L exposure heated to 130 K the average OH bend frequency appears at 938 cm^{-1} and shifts to 898 cm^{-1} at 150 K. From Table II, these frequencies suggest a transition from the β-polymorph to discrete HCOOH dimer pairs over this temperature range. The difference between these frequencies and those for their gas- and solid-phase counterparts can be attributed to perturbation from the surface. At this lower exposure (coverage) the perturbation per molecule is greater than on a surface exposed to more HCOOH owing to a lower level of lateral interaction between HCOOH adspecies.

2. Temperature and Coverage Dependence of Conversion of Molecular HCOOH to Bridging Formate. The vibrational information obtained from HREELS indicates both temperature and coverage dependences for the conversion of molecular HCOOH to bridging formate. For an exposure of 0.2 L, the decrease in the loss intensity for the molecular HCOOH out-of-plane OH bend and the concurrent increase in the loss intensity for the formate symmetric OCO stretch are both continuous between 130 K and 170 K. Beyond 170 K the OH bend loss is not observed and the OCO stretch loss reaches a maximum. At this exposure also, a very small amount of molecular desorption occurs between 200 K and 250 K.

We deduce a simple sequence of events which occurs at this exposure. At 80–100 K HCOOH adsorbs molecularly, with its plane parallel to the surface (or nearly so). Mobility of surface monomers allows the formation of hydrogen-bonded chains similar to the β-polymorph of solid HCOOH. Above 130 K the chains convert to discrete dimer pairs. In this form the HCOOH molecules begin to lose their hydroxyl protons to the surface, forming hydrogen adatoms; this is accompanied by formation of a bond between the surface and the carbonyl oxygen, yielding bridging formate. This conversion is complete by 170 K with almost all of the HCOOH reacting by this route.

For the surface exposed to 0.8 L HCOOH, the temperature dependence of the intensities of these losses is significantly changed. The loss intensity for the OH bend shows only a slight decrease before 140 K, followed by a sharp drop to a plateau between 160 K and 180 K, and finally extinction at 190 K. The loss for the OCO stretch appears above 140 K (10 K higher than at the lower exposure), and its intensity increases slowly up to 170 K. Above this, its intensity increases rapidly to a maximum at 190 K.

These data can be explained by considering the molecular desorption states and shift in OH bend frequency occurring at 0.8 L exposure. As noted previously, the OH bend frequency shifts by 40 cm^{-1} between 130 K and 150 K, indicating a transition from the α-polymorph to the β-polymorph. The resultant desorption must contribute to the dramatic drop in the molecular HCOOH loss intensity between 140 K and 160 K, although the data of Figure 8b suggest that there is simultaneous loss of the acid due to formate conversion. The increase of 10 K for the appearance of formate relative to the 0.2 L exposure could be explained by the α-to-β transition. The conversion from molecular HCOOH to formate could require a certain ensemble of surface atoms which is only available after transition to the less densely packed β-phase, or the orientation of the HCOOH molecules in the β-phase might allow conversion more readily than in the α-phase.

The coexistence of the plateau in the molecular HCOOH loss intensity with the continual increase in the formate loss intensity, shown in Figure 8, is more problematic. Consideration of possible coverage-dependent changes in the scattering cross sections for these vibrations makes any discussion somewhat speculative; however, a possible explanation might proceed as follows. The plateau between 160 and 180 K in Figure 8a suggests that deprotonation is complete by 160 K. Yet in this same temperature range the intensity of the formate-related loss rises, especially between 170 and 180 K, as shown by Figure 8b. Perhaps the increase in intensity of the formate feature in this temperature regime is due to reorientation from an almost-parallel configuration, to a perpendicular one where the OCO stretch is completely dipole-allowed. Reorientation may be inhibited at this high coverage by the coexistent molecular acid, owing to hydrogen bonding between the two adspecies. Above 170 K, the reorientation rate accelerates, implying a breakdown in the hydrogen bonding. Perhaps this acceleration is linked to desorption of molecular HCOOH at 200 K, although the constancy of the data in Figure 8a between 160 and 180 K suggests that desorption of the acid does not actually begin until 180–190 K in these experiments.

3. Coverage Dependence of Thermal Desorption States. Decomposition of bridging formate causes almost all the desorption observed from the surface exposed to 0.2 L HCOOH. This formate results from the reaction of discrete pairs of HCOOH dimers with the Pt(111) surface outlined above. This formate decomposes above 200 K giving CO_2 desorption peaked at 260 K, followed by desorption-limited H_2 centered at 350 K. There is also a small amount of molecular desorption which roughly follows the CO_2 desorption. Considering that bridging formate is the only adspecies observed in the vibrational spectra above 170 K, this molecular desorption must arise from recombination of formate and H adatoms.

Increasing the exposure to 0.8 L HCOOH populates two molecular desorption states. The desorption spectra for masses 29 and 47 exhibit these states centered at 160 K and 200 K, but the relative intensities of these states are different in the two spectra. This suggests that there are two different forms of molecular HCOOH desorbing, namely, monomers and dimers. The 160 K state in the mass 47 spectrum is six times as intense as the 200 K state (mass 47 is the molecular weight of one HCOOH molecule plus one proton). The 200 K state in the mass 29 spectrum is three times larger than the 160 K state. We suggest that desorption from the 160 K state is dominated by HCOOH dimers and that from the 200 K state by HCOOH monomers. Additionally, at high HCOOH exposures (>2.3 L), we observe broad desorption features in mass 91 spectra (not shown) centered between 160 K and 170 K; we believe this further supports the predominance of dimers in the lower temperature desorption state, although we cannot rule out desorption of higher oligomers. (Mass 91 is the molecular weight of a formic acid dimer missing a proton.)

Two scenarios could explain the differences in the two molecular desorption states. (1) Desorption from the 160 K state is from a second layer with no HCOOH in direct contact with the surface. The presence of this second layer constrains the HCOOH in contact with the surface to the α-polymorph configuration. Heating the surface beyond 140 K desorbs the second layer in the form of HCOOH dimers and allows the first layer HCOOH to convert to the β-polymorph, with subsequent reaction to form bridging formate. (2) Desorption from the 160 K state is from HCOOH in direct contact with the surface. Such an overlayer would be in the denser α-polymorph. Heating this surface beyond 140 K would cause rupture of the hydrogen-bonded chains, squeezing out HCOOH dimers and allowing conversion to the β-polymorph.

We can extract from the second model an explanation to support immediate deprotonation of HCOOH upon α-to-β conversion.

(38) Holtzberg, F.; Post, B.; Fankuchen, I. *Acta Crystallogr.* **1953**, 6, 127.

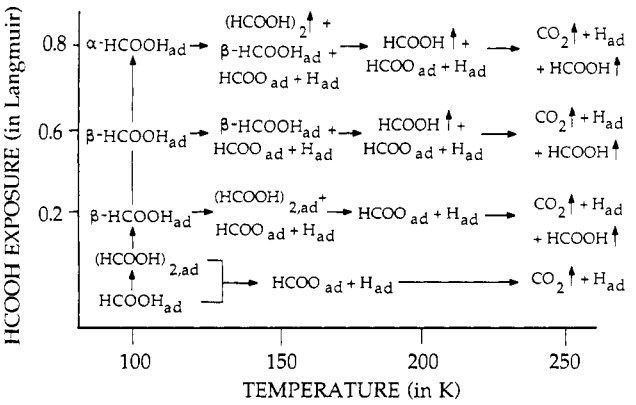

Figure 10. Summary of the coverage dependence of the HCOOH overlayer for adsorption at 80–100 K and its temperature dependence for conversion to formate for different coverages.

Rupture of the hydrogen-bonded chains via dimer displacement would result in a higher number of terminal HCOOH molecules. Chain rupture could be followed or accompanied by deprotonation of these terminal molecules; reorientation would be slowed by their continued interaction with linking HCOOH molecules in the shortened chains.

5. Conclusions

The scheme for the reaction of HCOOH with Pt(111) is summarized in Figure 10. For extremely low exposures at 80–100 K, we posit that HCOOH exists molecularly as monomers or discrete dimer pairs. As surface temperature increases, the acid deprotonates to produce bridging formate and hydrogen adatoms. As exposure increases at 80–100 K, the population of HCOOH reaches a level sufficient to form hydrogen-bonded chains in a configuration similar to the solid-phase β-polymorph. This is the surface condition we observe for an exposure of 0.2 L. Heating this overlayer to 150 K causes reversion to discrete dimer pairs, followed by conversion to bridging formate. By 170 K, conversion is complete. Between 200 K and 250 K a small amount of formate recombines with atomic hydrogen to desorb molecularly; however, the majority of formate decomposes, resulting in CO_2 desorption peaking at ~260 K.

We believe the β-polymorph remains the preferred configuration for HCOOH adsorbed at 80–100 K up to an exposure which populates the second molecular desorption state (0.6 L); however, at higher exposures the hydrogen-bonded chains resemble the denser α-polymorph. Heating the surface above 130 K transforms the α-phase to the β-phase; this is tied to the second molecular HCOOH desorption state. Desorption results from depopulation of a second layer or rupture of first-layer chains; the desorption products are gaseous dimers. A fraction of the HCOOH which remains in the overlayer immediately deprotonates and reorients to a perpendicular, bridging configuration with increasing surface temperature. The HCOOH which does not deprotonate desorbs from the surface (peaked at 200 K) as monomers.

Increasing exposure from 0.2 L to 0.6 L changes the pathway of formate formation. As described above for 0.2 L HCOOH exposure, production of formate is preceded by the reversion of HCOOH chains to discrete dimer pairs. Increasing coverage eventually prevents this reversion, leading to formate production directly from HCOOH chains and desorption of molecular HCOOH peaked at 200 K. Subsequent formate decomposition proceeds as for the 0.2 L exposure.

Acknowledgment is made to the donors of the Petroleum Research Fund, administered by the American Chemical Society, for the support of this research. Some equipment and all facilities are provided by the Ames Laboratory, which is operated for the U.S. Department of Energy by Iowa State University under Contract No. W-7405-ENG-82.

Registry No. HCOOH, 64-18-6; Pt, 7440-06-4; formate, 71-47-6.

Gas-Phase Oxidation of Group 6 Metal Carbonyl Anions

C. E. C. A. Hop† and T. B. McMahon*

Contribution from the Department of Chemistry and Guelph-Waterloo Centre For Graduate Work in Chemistry, University of Waterloo, Waterloo, Ontario N2L 3G1, Canada.
Received June 24, 1991

Abstract: Oxidation of $Cr(CO)_5^-$, $Mo(CO)_5^-$, and $W(CO)_5^-$ was examined in a low-pressure (~5×10^{-8} mbar) and a high-pressure (~3.5 mbar) environment using a Fourier-transform ion cyclotron resonance spectrometer equipped with a high-pressure external ion source. Although the oxidation chemistry displayed by the Cr and W systems was fairly similar, the Mo analogue had several unique features. In addition, remarkable differences were observed between high- and low-pressure oxidation. For example, MO_5^- ions were only generated under high-pressure conditions. This indicates that generation of MO_5^- ions requires termolecular reactions. Alternatively, it could be that the intermediate for generation of MO_5^- has a very short lifetime and dissociates prior to reaction with O_2 under low-pressure conditions. Energy-resolved collision-induced dissociation was used to obtain structural information about the various product ions, and it allowed determination of bond strengths in these ions. The experiments revealed that for all the $M(CO)_xO_2^-$ (x = 3, 4) product ions the two oxygen atoms are bound as two separate oxo ligands and not as a dioxygen ligand. The MO_5^- ions contain two (or possibly one) O_2 molecules bound as peroxo or superoxo ligands.

Introduction

Transitional metals play an important role in organic and inorganic chemistry and biochemistry.[1] The transition-metal oxides are of particular importance because of their involvement as catalysts in oxidation of organic substrates.[2] Transition-metal compounds containing a dioxygen ligand[3] are especially effective

† Present address: Department of Chemistry, University of Wisconsin—Madison, Madison, Wisconsin 53706.

(1) (a) Cotton, F. A.; Wilkinson, G. *Advanced Inorganic Chemistry*; John Wiley & Sons: New York, 1980. (b) Collman, J. P.; Hegedus, L. S.; Norton, J. R.; Finke, R. G. *Principles and Applications of Organotransition Metal Chemistry*; University Science Books: Mill Valley, 1987.

0002-7863/92/1514-1237$03.00/0